J Solid State Electrochem (2016) 20:47–54
DOI 10.1007/s10008-015-3003-8

ORIGINAL PAPER

Amperometric tyrosinase biosensor based on boron-doped nanocrystalline diamond film electrode for the detection of phenolic compounds

Yousheng Zou[1] · Dong Lou[1] · Kang Dou[1] · Linlin He[1] · Yuhang Dong[1] · Shalong Wang[1]

Received: 27 May 2015 / Revised: 28 July 2015 / Accepted: 31 July 2015 / Published online: 9 August 2015

Abstract A novel tyrosinase amperometric biosensor based on boron-doped nanocrystalline diamond (BDND) film electrode has been developed for the detection of phenolic compounds. Amine-terminated BDND surface was achieved via a direct photochemical reaction with allylamine. The tyrosinase was then covalently immobilized on the amine-terminated diamond film electrode surface. The effects of pH and applied potential on the performance of tyrosinase amperometric biosensor were investigated. The biosensor showed an optimum response at a pH of 6.5 and at an applied potential of −100 mV. It also exhibited good analytical performances to phenolic compounds in terms of sensitivity, detection limit, and stability. The tyrosinase-modified BDND film electrode exhibited a rapid response to the changes in the substrate concentration for all the phenolic compounds tested and reached 95 % of steady-state current in about 10 s. It is attributed to the high loading of tyrosinase and the rapid electron transfer between the tyrosinase and BDND film electrode surface. The tyrosinase-modified BDND film electrode showed high sensitivity with 184.0, 95.6, and 552.3 mA M^{-1} cm^{-2} and a linear response range of 10.0–120.0, 5.0–120.0, and 30.0–120.0 μM for phenol, catechol, and 4-chlorophenol, respectively.

Keywords Boron-doped nanocrystalline diamond film · Tyrosinase · Amperometric biosensor · Phenolic compounds

✉ Yousheng Zou
yshzou75@mail.njust.edu.cn

[1] School of Materials Science and Engineering, Institute of Optoelectronics and Nanomaterials, Nanjing University of Science and Technology, Nanjing, Jiangsu 210094, China

Introduction

Phenolic compounds are widely used chemicals and released into the environment by a large number of industrial and agricultural activities [1, 2]. Meanwhile, most of phenolic compounds show harmful effects on human health or the environment due to their toxicity. Therefore, the rapid and accurate determination and the control of phenolic compounds are of great importance. So far, several analytical techniques, such as fluorescence quenching [3], capillary electrophoresis [4, 5], high-performance liquid chromatography (HPLC) [6], and electrochemistry methods have been developed for detecting the phenolic compounds [7–9]. However, the conventional photometric and chromatographic methods require complicated pretreatment procedures and are very expensive, time-consuming, and unsuitable for on-site monitoring. Therefore, significant efforts have been made for developing simple, effective, and sensitive analytical methods for detecting phenolic compounds. This then prompted the development of amperometric biosensors based on polyphenol oxidase which are inexpensive, disposable, and highly sensitive for detecting phenolic compounds in environmental and biological samples to overcome these drawbacks [10–14].

Enzyme-based amperometric biosensors that combine the high specificity of enzymes with the sensitivity and accuracy of electrochemical indicator reactions have been widely used as bioelectrocatalyst for detecting phenolic compounds. Among them, tyrosinase is the most widely used enzyme [15–17]. Tyrosinase is a binuclear copper metalloprotein that catalyzes the oxidation of monophenols by molecular oxygen to form *o*-biphenols, which are subsequently oxidized to *o*-quinones [18, 19]. The general performance of this sort of biosensor depends on the activity of the enzyme that is secured by the polymeric matrix onto the electrode surface. Therefore, the effective immobilization of tyrosinase on the

electrode surface is a key step in the construction of tyrosinase biosensors. Different approaches for tyrosinase immobilization, such as physical adsorption [20], covalent cross-linking [21, 22], incorporation within carbon paste [23, 24], immobilization in polymer films [25], entrapment in cryo-hydrogel, and some sol-gel matrices have been widely used to construct tyrosinase biosensors [26–28].

On the other hand, the enzyme-based amperometric biosensor performance also largely depends on the electrode materials. Various matrices, including carbon nanotube, nafion membrane, hydrogel, graphite, conducting polymers, and biopolymers have been used in the construction of sensor probes [29–32]. The electrochemical tyrosinase biosensor based on a tyrosinase-nano-hydroxyapatite-chitosan bio-nanocomposite biosensor exhibited a linear response to catechol over a wide concentration range from 10 nM to 7 μM, with a high sensitivity of 2.11×10^3 μA mM^{-1} cm^{-2} and a detection limit of 5 nM [33]. A sandwich-type phenolic biosensor based on wrapping tyrosinase into single-walled carbon nanotubes (SWCNTs) and polyaniline (PANI) nanocomposites exhibited a good analytical performance for the amperometric detection of phenolic compounds due to synergistic effect of SWCNTs and PANI [11]. In electroanalytical chemistry, boron-doped diamond film has increasingly been used as an excellent electrode material due to its unique properties, such as wide electrochemical potential window, low background current, superb electrochemical stability in aqueous solution, excellent adsorption resistance, as well as good biocompatibility, which outperform the traditional carbon materials. Boron-doped diamond film electrode has been demonstrated to enhance stability and sensitivity of electrochemical detection of phenolic compounds. Zhao et al. [34] developed a tyrosinase biosensor based on biofunctional ZnO nanorod microarrays on diamond film electrode and observed the high sensitivity and stability for the amperometric detection of phenolic compounds. The tyrosinase-AuNPs/boron-doped diamond biosensor fabricated by immobilizing tyrosinase on AuNPs electrodeposited on a boron-doped diamond electrode exhibited good sensitivity, stability, and reproducibility for the determination of phenol [35].

In this paper, the tyrosinase amperometric biosensors based on boron-doped nanocrystalline diamond (BDND) film electrode were fabricated and then used for the detection of phenolic compounds. The amination of hydrogen-terminated BDND film surfaces was firstly performed by direct photochemical method, and then tyrosinase was covalently immobilized onto the amine-terminated diamond film surface by cross-linking with glutaraldehyde. The morphology and electrochemical properties of the tyrosinase-modified BDND films were studied. The tyrosinase amperometric biosensor performances including sensitivity, linear range, limits of detection, and stability have been investigated in detail.

Experimental

Chemical and reagents

Tyrosinase (25 KU mg^{-1}) and glutaraldehyde (GA, 25 % water solution) were purchased from Sigma. Phenol (AR grade), catechol (AR grade), 4-chlorophenol (AR grade), and allylamine were purchased from Shanghai Chemical Company (Shanghai, China). These phenolic compounds were prepared by dissolving appropriate amount in a 0.1 M PBS prepared by using Na_2HPO_4 and KH_2PO_4. Ultrapure water produced by a simple laboratory water system (Millipore) was used in the experiment.

Preparation of the tyrosinase-modified BDND film electrode

Boron-doped nanocrystalline diamond films were deposited on Si (100) substrate by commercial ASTeX microwave plasma CVD (MWCVD) reactor equipped with a 1.5-kW microwave generator using CH_4 and trimethylboron (TMB) diluted in H_2. The substrates were ultrasonically abraded for 60 min in a suspension of mixed diamond powders with a grain size of 5 nm and 3 μm in ethanol to obtain high nucleation density. The plasma was induced in a gas mixture of 10 % CH_4/90 % (H_2 and TMB) with a microwave power of 1200 W and total pressure of 30 Torr. The substrate temperature was maintained at approximately 800 °C, and the boron-carbon ratio (B/C) in the feed gas mixture was kept to 5000 ppm. The deposition time was fixed at 6 h. The surface morphology and phase composition of the deposited BDND films were characterized by scanning electron microscopy and visible Raman spectroscopy.

Then the surface of as-deposited BDND films was covalently functionalized with amine group, which has been shown in detail in our previous report [36]. Briefly, the allylamine was first dipped onto the as-deposited BDND film surface in a nitrogen-purged teflon reactor covered with a quartz window. Then the sample was illuminated through the quartz window with the 254-nm UV lamp for 12 h. After illumination, the amine group-modified BDND films were ultrasonically cleaned in ethanol and deionized water, respectively.

The tyrosinase-modified BDND film electrode was prepared as follows: 100 μL of 25 KU mg^{-1} tyrosinase solution was dispersed onto the surface of the amine-terminated BDND film electrode, and then 30 μL of 2.5 % glutaraldehyde solution was added. Then the resulting BDND film electrode was stored for 12 h at 4 °C so that the tyrosinase could be sufficiently immobilized onto the surface of the amine-modified BDND film electrode. The resulting enzyme-modified electrode was thoroughly rinsed with buffer solution

to remove any unbound enzyme molecules and preserved in 0.1 M PBS (pH = 6.5) at 4 °C until required.

Electrochemical measurements

The electrochemical measurements were performed on a CHI660E electrochemical workstation (Shanghai Chenhua, China) in a conventional three-electrode cell system. The tyrosinase-modified BDND film electrode was used as a working electrode. A platinum wire and a saturated calomel electrode (SCE) were used as counter electrode and reference electrode, respectively. All the electrochemical experiments were conducted at room temperature.

Results and discussion

Figure 1a shows the plain-view SEM image of the BDND film deposited at B/C = 5000 ppm. It can be seen that the film is continuous and composed of nanograins. The grains gather together forming hillock-like clusters with inhomogeneous size. The phase composition of BDND film was examined by visible Raman spectroscopy. As shown in Fig. 1b, four peaks located at around 500, 1220, 1305, and 1490 cm^{-1} in the visible Raman spectra were observed. The peaks around 500 and 1220 cm^{-1} become the main features with respect to the undoped nanocrystalline diamond film, indicating the characteristic for highly boron-doped diamond. Moreover, the characteristic peak for diamond at 1332 cm^{-1} downshifts to about 1305 cm^{-1} due to the heavy boron doping. The presence of the band at 500 and 1220 cm^{-1} is associated with the Fano effect interference between the zone center Raman active optical phonon and the continuum of electronic states induced by the presence of the boron dopant [37]. In addition, the highly reliable commercial MWCVD system used in the present work is capable of depositing high-quality BDND films with reproducible sample quality.

The lack of chemically reactive groups precludes from the attachment of biomolecules to the diamond surface. Surface termination is considered to be an effective approach to modulating the properties of a diamond surface by introducing diverse terminals such as −OH, $-NH_2$, and −COOH. Among these functionalized terminals, amine ($-NH_2$) groups have been widely used as tethering sites for immobilization of biomolecules onto the diamond surface [38–41]. Thus, to immobilize the tyrosinase on the diamond surface, the direct surface functionalization of BDND film surface with amine groups was firstly achieved by reacting with allylamine molecules under UV light irradiation. The detailed procedure was described, and the corresponding XPS analysis confirmed the presence of stable amino groups immobilized on BDND film surface in our previous work [36]. The tyrosinase was then immobilized on the BDND film electrode surface by cross-linking with glutaraldehyde, and the morphology was characterized by SEM. Figure 2 shows the SEM image obtained from the tyrosinase-modified BDND film electrode. It can be observed that the particles with inhomogenous shape and size are distributed throughout the tyrosinase-modified BDND film electrode surface. These irregularly shaped particles are assigned to tyrosinase molecules. In addition, we also observed that the BDND film morphology is unaffected after animation. There is no SEM image difference for the BDND film was found after modification with allylamine molecules.

The electrochemical behavior of the different BDND film electrode was evaluated by the analysis of redox couples of $[Fe(CN)_6]^{3-/4-}$, as shown in Fig. 3. Well-defined and symmetric CV curves of $[Fe(CN)_6]^{3-}/[Fe(CN)_6]^{4-}$ on the as-deposited and modified BDND film electrodes were obtained. The anodic peak potential to cathodic peak potential separations (ΔE_p) for the as-deposited, amine-terminated, and tyrosinase-modified BDND film electrodes is about 70, 87, and 97 mV, respectively. It indicates that there is a nearly reversible or quasi-reversible electrode reaction of $K_3Fe(CN)_6$ on the surface of BDND film electrodes. Compared with the as-deposited BDND film electrode, however, increased ΔE_p were observed for the amine-terminated and tyrosinase-modified BDND film electrodes. Moreover, the separation of peak to peak increases following this sequence: ΔE_p(tyrosinase-modified BDND) > ΔE_p(amine-terminated BDND) > ΔE_p(as-deposited BDND), indicating that the presence of amine layer and tyrosinase on the BDND surface resulted in the increase of resistance to the electron transfer.

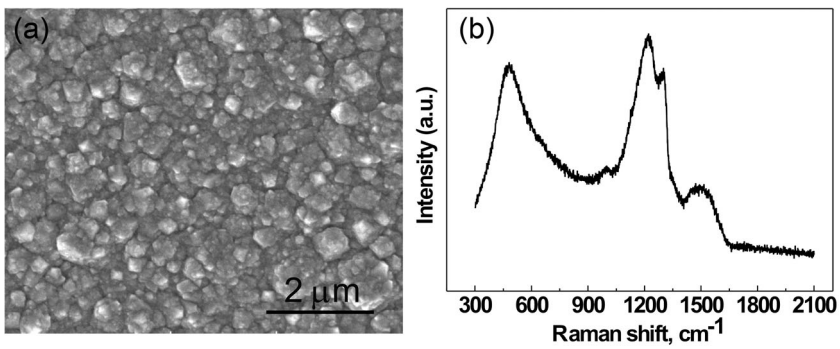

Fig. 1 **a** SEM image and **b** Raman spectra of as-deposited BDND film electrode

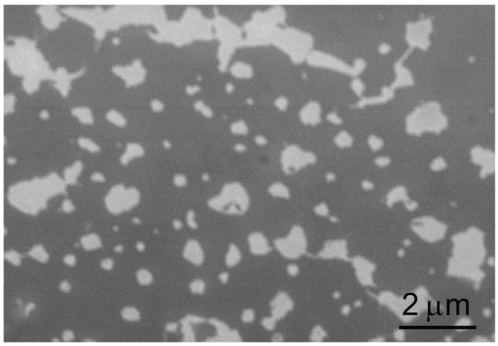

Fig. 2 Surface SEM image obtained from the tyrosinase-modified BDND film electrode

Similar results were also reported for the tyrosinase-modified boron-doped diamond film electrode by Zhou [42].

Electrochemical impedance spectrum (EIS) is a powerful tool for studying the interface properties of working electrode. The impedance measurements of the three different BDND film electrodes were carried out at the open circuit potential in 1 M KCl solution containing 1 mM $K_3Fe(CN)_6$ over a frequency range of 1×10^{-2} to 1×10^{5} Hz. From Fig. 4, it can be seen that the impedance spectra includes a semicircular portion at higher frequency corresponding to the electron transfer limited process and a linear portion at lower frequency representing the diffusion-controlled process. The effective diameter of the semicircle corresponding to the electron transfer resistance increases after the modification of BDND film electrode, as shown by the curves b and c in Fig. 4. In comparison with as-deposited and amine-terminated BDND film electrode, the tyrosinase-modified BDND film electrode exhibits the largest electron transfer resistance, indicating the slowest electron transfer rate between the Pt electrode and BDND film electrode, which is consistent with the results of Fig. 3. The increase of electron transfer resistance of tyrosinase-modified BDND film electrode might be attributed to the non-conductive tyrosinase on diamond surface, which hinders electron transfer of the electrochemical probe. The

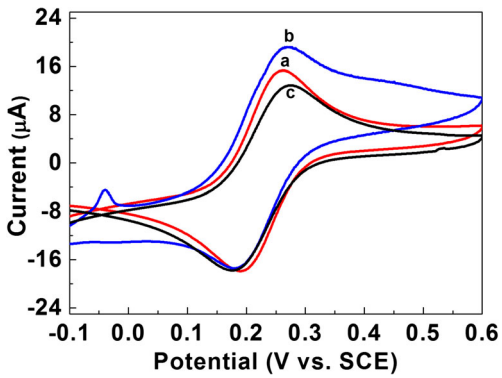

Fig. 3 Cyclic voltammograms of 1 mM $K_3Fe(CN)_6$ in 1 M KCl solution at the scanning rate of 60 mV s^{-1} obtained at as-deposited BDND film electrode (*curve a*), amine-terminated BDND film electrode (*curve b*), and tyrosinase-modified BDND film electrode (*curve c*)

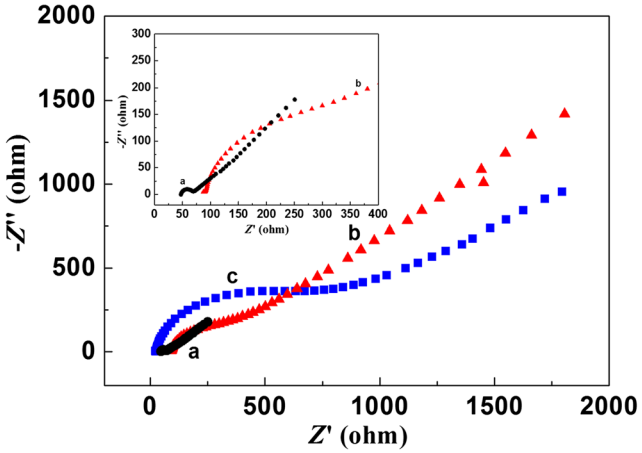

Fig. 4 Nyquist plots of EIS of 1 mM $K_3Fe(CN)_6$ in 1 M KCl solution at open circuit potential for as-deposited BDND film electrode (*curve a*), amine-terminated BDND film electrode (*curve b*), and tyrosinase-modified BDND film electrode (*curve c*). *Inset* shows the enlargement of *curves a* and *b*

results of EIS confirm successful immobilization of tyrosinase on diamond surface.

Figure 5 shows the CVs obtained from various BDND film electrodes in 0.1 M PBS (pH = 6.5) solution with the addition of 0.4 mM catechol at the scanning rate of 60 mV s^{-1}. For the as-deposited and amine-terminated BDND film electrodes without enzyme, there was no reduction peak of the CVs besides the low background current. However, a well-defined peak located at about −0.03 V in the CV was observed for the tyrosinase-modified BDND film electrode. It was due to the reduction of enzymatically produced *o*-quinone species liberated from the enzymatic reaction on the BDND film electrode surface. The enzymatic product *o*-quinone is generated during the course of tyrosinase-catalyzed oxidation of catechol in the presence of dissolved oxygen. The steps of the enzymatic reaction on the modified BDND film electrode surface were shown as follows [43]:

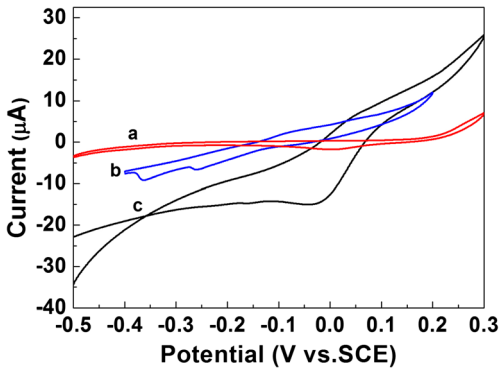

Fig. 5 Cyclic voltammograms of 0.4 mM catechol in 0.1 M PBS (pH = 6.5) solution at the scanning rate of 60 mV s^{-1} obtained at as-deposited BDND film electrode (*curve a*), amine-terminated BDND film electrode (*curve b*), and tyrosinase-modified BDND film electrode (*curve c*)

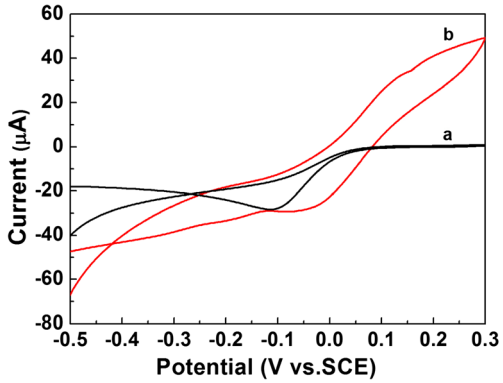

Fig. 6 Cyclic voltammograms of 0.14 mM phenol (*curve a*) and 0.32 mM 4-chlorophenol (*curve b*) in 0.1 M PBS (pH = 6.5) solution at the scanning rate of 60 mV s^{-1} obtained at the tyrosinase-modified BDND film electrode

$$\text{catechol} + \text{tyrosin}ase\,(O_2) \rightarrow o\text{−quinone} + H_2O \quad (1)$$

$$o\text{−quinone} + 2H^+ + 2e^- \rightarrow \text{catechol}\,(at\ \text{electrode}) \quad (2)$$

Similar to the catechol, the well-defined peak in the CVs was also observed when detecting the phenol and 4-chlorophenol for the tyrosinase-modified BDND film electrode, as shown in Fig. 6. The CV results show that the immobilization process retains the biological activity of tyrosinase on the modified BDND film electrode. This indicated that phenolic compounds, such as phenol, catechol, and 4-chlorophenol, can be detected by using tyrosinase amperometric biosensor based on BDND film electrode.

It is well known that the tyrosinase enzyme activities strongly depend on the pH value of buffer solution. Therefore, the effect of pH on the performance of the tyrosinase-modified BDND film electrode was investigated. Figure 7 shows the pH dependence of the amperometric response of 0.4 mM catechol in the pH range of 5.5–7.5. It can be seen that the reduction current density increases as the pH increases from 5.5 to 6.5 due to the increasing of tyrosinase activity and then decreases gradually as pH increases further from 6.5 to 7.5. The decrease of the amperometric response at pH over 6.5 was due to the involvement of protons in the reduction reaction of *o*-quinone. The reduction current density reaches the maximum at a pH of 6.5. The results indicated an optimum sensor response at a solution pH of 6.5, which is in good agreement with the optimum pH value obtained for tyrosinase by others [42, 44]. Therefore, the pH of 6.5 for the PBS was selected for the following studies to obtain the maximum response.

The effect of applied potential on the performance of the tyrosinase-modified BDND film electrode was also investigated. Figure 8 shows the effect of applied potential on the amperometric signal (curve b), the background current (curve a), and the ratio of signal to noise (curve c) in 0.1 M PBS (pH = 6.5) containing 0.4 mM catechol for the tyrosinase-modified BDND film electrode. It can be seen that the background current increases when the applied potential is more negative in the range between 50 mV and −300 mV. However, the amperometric signal current increases rapidly and then decreases slightly when the applied potential increases from 50 to −300 mV. A maximum ratio of signal to background current for the tyrosinase-modified BDND film electrode is obtained at −100 mV (vs. SCE). Moreover, low applied potential can minimize interferences from electroactive species. The decrease of the response at more negative potentials was due to the decrease in the tyrosinase enzymatic rate resulting from the oxygen depletion in the vicinity of the tyrosinase immobilized at the electrode surface. Thus, the applied potential of −100 mV was applied for the following experiments.

Figure 9 shows the current-time recording curve for the tyrosinase-modified BDND film electrode to different phenolic compounds on the successive step addition of phenol, catechol, and 4-chlorophenol under the optimized experimental conditions. A well-defined reduction current proportional to the concentration of phenolic compounds is observed. The tyrosinase-modified BDND film electrode exhibited a rapid bioelectrocatalytic response to the change of substrate concentration and reached 95 % of steady-state current in less than 10 s because of the high loading of tyrosinase and the rapid

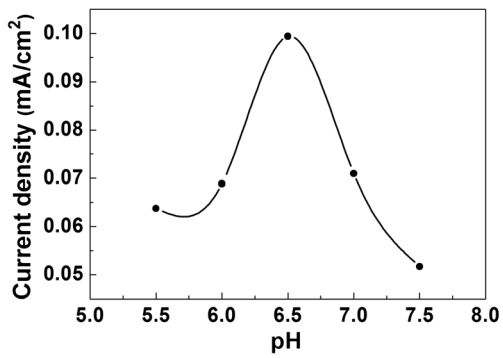

Fig. 7 The effect of pH value in 0.1 M PBS containing 0.4 mM catechol on the obtained current density at the tyrosinase-modified BDND film electrode

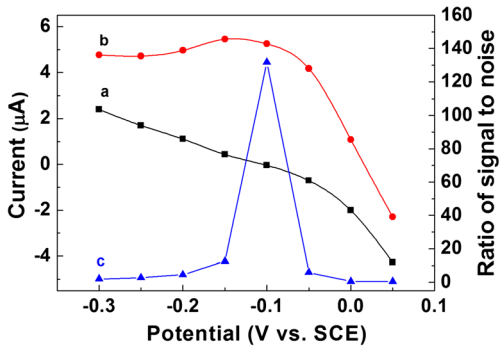

Fig. 8 The effect of applied potential on the amperometric signal (*curve b*), background current (*curve a*), and the ratio of signal to noise (*curve c*) in 0.1 M PBS (pH = 6.5) containing 0.4 mM catechol for the tyrosinase-modified BDND film electrode

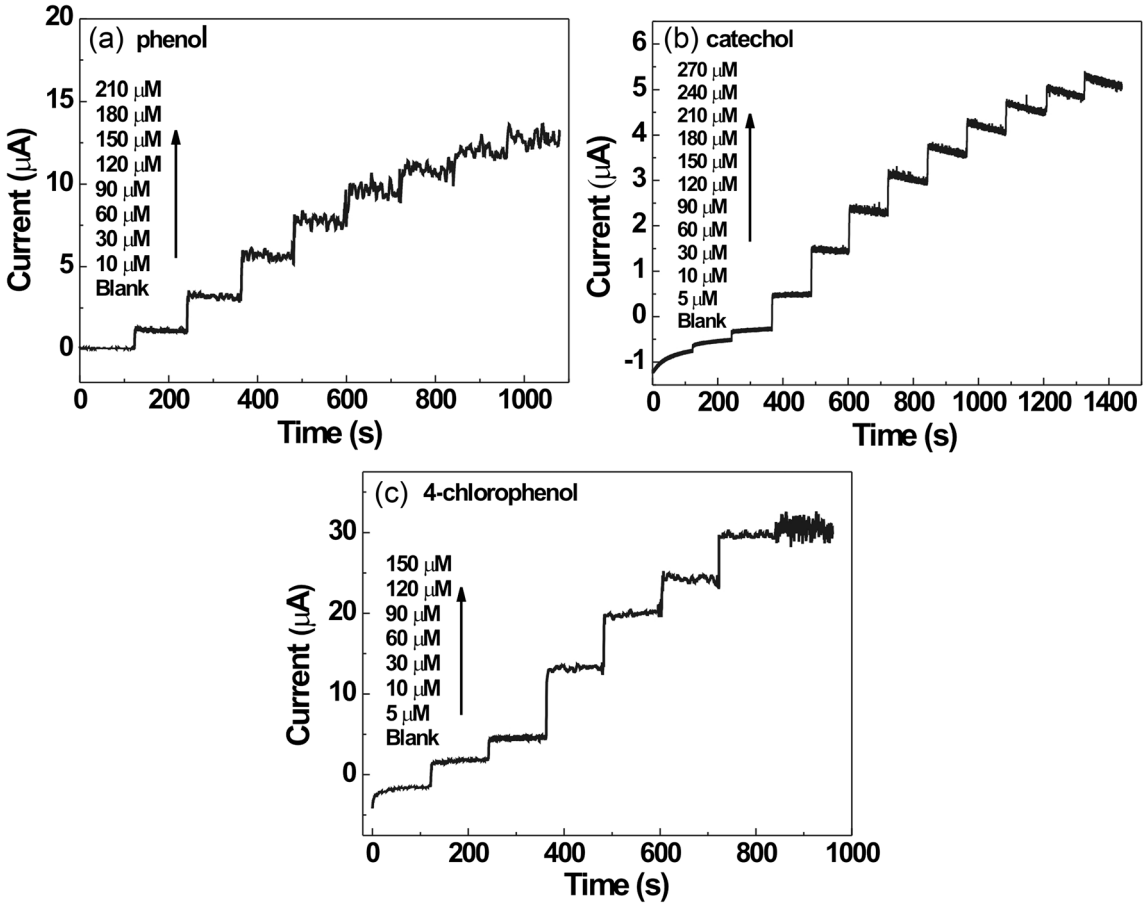

Fig. 9 Current-time recordings curve of the tyrosinase-modified BDND film electrode to different phenolic compounds in 0.1 M PBS (pH = 6.5), **a** phenol, **b** catechol, and **c** 4-chlorophenol

electron transfer between the quinones and the electrode surface. The response of our tyrosinase amperometric biosensor based on BDND film is close to that of 8 s reported in a tyrosinase-nano-hydroxyapatite-chitosan bio-nanocomposite towards catechol [45] and much faster than that of 30 s reported in a conducting polymer film [46].

Figure 10 shows the typical calibration curves of the tyrosinase-modified BDND film electrode towards phenol, catechol, and 4-chlorophenol. The response characteristics of tyrosinase-modified BDND film electrode to various phenolic compounds extracted from Fig. 10 are listed in Table 1. The linearity of the tyrosinase-modified BDND film electrode towards phenol, catechol, and 4-chlorophenol was achieved in the concentration range of 10.0–120.0, 5.0–120.0, and 30.0–120.0 μM, respectively. This dynamic range of monitoring phenolic compounds is much wider than the previously

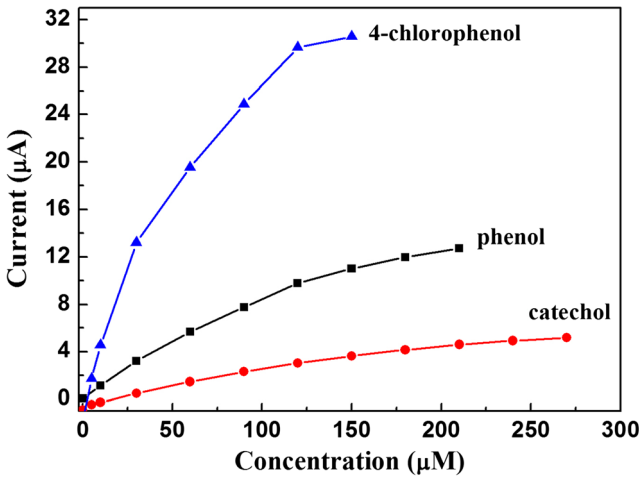

Fig. 10 Calibration curves of the tyrosinase-modified BDND film electrode to phenol, catechol, and 4-chlorophenol; supporting electrolyte 0.1 M PBS (pH = 6.5); applied potential −100 mV

Table 1 Response characteristics of the tyrosinase-modified BDND film electrode to phenolic compounds

Phenolic compound	Liner range (μM)	Sensitivity (mA M^{-1} cm^{-2})	Detection limit (μM)	Correlation coefficient
Phenol	10–120	184	2.33	0.9915
Catechol	5–120	95.6	3.28	0.9919
4-Chlorophenol	30–120	552.3	1.19	0.9936

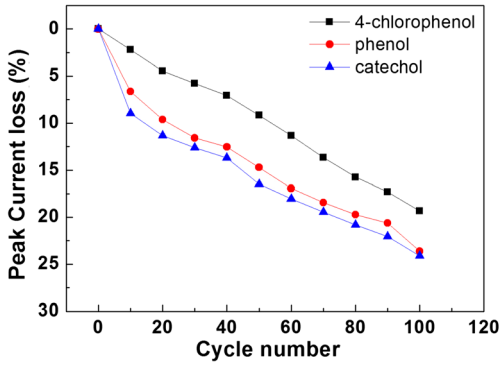

Fig. 11 The electrochemical cycling stability of the tyrosinase-modified BDND film electrode for phenol, catechol, and 4-chlorophenol in 0.1 M PBS (pH = 6.5)

reported biosensors, where the dynamic range is less than 100 μM for phenol and 50 μM for other phenolic compounds [47, 48]. The limits of detection were determined to be 2.33, 3.28, and 1.19 μM for phenol, catechol, and 4-chlorophenol, respectively. The tyrosinase-modified BDND film electrode also exhibited high sensitivity with 184.0, 95.6, and 552.3 mA M^{-1} cm^{-2} for phenol, catechol, and 4-chlorophenol, respectively. Moreover, the sensitivity for the linear calibration regions decreases in the following sequence: 4-chlorophenol > phenol > catechol. The difference in sensitivity might depend on the tyrosinase catalytic selectivity for different phenolic compounds. The 4-chlorophenol at tyrosinase-modified BDND film electrode shows the minimum detection limit and maximum sensitivity.

The stability of the tyrosinase-modified BDND film electrode was also studied through the current response to various phenol compounds in 0.1 M PBS at −100 mV. From Fig. 11, it can be observed that the peak current decreases quickly at the initial 10 cycles and then decreases gradually. According to the decrease of peak current, the loss of the electrochemical activity for 4-chlorophenol, phenol, and catechol was found to be about 19.4, 23.6, and 24.1 %, respectively, after 100 repetitive cycles. The results of stability indicated that the tyrosinase-modified BDND film electrode was relatively stable owing to the inertness of the diamond surface.

Conclusion

A sensitive tyrosinase biosensor for the determination of phenolic compounds (phenol, catechol, and 4-chlorophenol) was constructed based on covalent immobilization of tyrosinase onto BDND film deposited by MWCVD. A homogeneous layer of amine groups was bonded covalently to the diamond surface via a direct photochemical reaction with allylamine. The tyrosinase was then immobilized onto the amine-terminated diamond film surface by cross-linking with glutaraldehyde. The response dependences of the tyrosinase-modified BDND film electrode on pH of solution and applied potential were studied in detail. The biosensor showed an optimum response at a pH of 6.5 and at an applied potential of −100 mV. The electrochemical tyrosinase biosensor provides a suitable microenvironment for retaining high bioactivity of tyrosinase and exhibits a good analytical performance for the amperometric detection of phenolic compounds in terms of linear range, detection limit, response time, and sensitivity. The results of amperometric response measurements on tyrosinase-modified BDND film electrode show high sensitivity with 184.0, 95.6, and 552.3 mA M^{-1} cm^{-2} and a broad linear response range of 10.0–120.0, 5.0–120.0, and 30.0–120.0 μM for phenol, catechol, and 4-chlorophenol, respectively. The minimum detection limit and maximum sensitivity were obtained for the 4-chlorophenol at a tyrosinase-modified BDND film electrode.

Acknowledgments This work was financially supported by the Natural Science Foundation of Jiangsu Province of China (BK20141401) and the Fundamental Research Funds for the Central Universities (30920130111019).

References

1. Luthria D, Singh AP, Wilson T, Vorsa N, Banuelos GS, Vinyard BT (2010) Food Chem 121:406–411
2. Andrade LS, Rocha-Filho RC, Bocchi N, Biaggio SR, Iniesta J, Garcia-Garcia V, Montiel V (2008) J Hazard Mater 153:252–260
3. Yeh YL, Yeh KJ, Hsu LF, Yu WC, Lee MH, Chen TC (2014) J Hazard Mater 277:27–33
4. Turkia H, Sirén H, Penttilä M, Pitkänen JP (2013) J Chromatogr A 1278:175–180
5. Wang HL, Yan H, Wang CJ, Chen F, Ma MP, Wang WW, Wang XD (2012) J Chromatogr A 1253:16–21
6. Jing X, Zhang X, Bao J (2009) Appl Biochem Biotechnol 159:696–707
7. Poerschmann J, Zhang ZY, Kopinke FD, Pawliszyn J (1997) Anal Chem 69:597–600
8. Omuro Lupetti K, Rocha FRP, Fatibello-Filho O (2004) Talanta 62: 463–467
9. Kovács A, Mortl M, Kende A (2011) Microchem J 99:125–131
10. Şenyurt Ö, Eyidoğan F, Yilmaz R, Tufan Öz M, Cengiz Özalp V, Arica Y, Öktem Hüseyin A (2015) Biotechnol Appl Biochem 62: 1332–1136
11. Wang BN, Zheng JB, He YP, Sheng QL (2013) Sensor Actuators B 186:417–422
12. Yang LJ, Xiong HY, Zhang XH, Wang SF (2012) Bioelectrochemistry 84:44–48
13. Hashemnia S, Khayatzadeh S, Hashemnia M (2012) J Solid State Electrochem 16:473–479
14. Stoytchev M, Zlatev R, Goche V, Velkov Z, Montero G, Beleño MT (2014) Electrochim Acta 147:25–30
15. Qu Y, Ma M, Wang ZG, Zhan GQ, Li BH, Wang X, Fang HF, Zhang HJ, Li CY (2013) Biosens Bioelectron 44:85–88
16. Han E, Yang Y, He Z, Cai J, Zhang X, Dong X (2015) Anal Biochem 486:102–106
17. Apetrei C, Rodriguez-Mendez ML, De Saja JA (2011) Electrochim. Acta 56:8919–8925

18. Pérez JPH, López MSP, Lopez-Cabarcos E, Lopez-Ruiz B (2006) Biosens Bioelectron 22:429–439
19. Yildiz HB, Castillo J, Gushin DA, Toppare L, Schumann W (2007) Microchim. Acta 159:27–34
20. Shiddiky MJA, Torriero AAJ (2011) Biosens Bioelectron 26:1775–1787
21. Takashima RW, Kaneto K (2004) Sensor Actuators B 102:271–277
22. Karim MN, Lee HJ (2013) Talanta 116:991–999
23. Kumar Vashist S, Zheng D, Al-Rubeaan K, Luong JHT, Sheu FS (2011) Biotechnol Adv 29:169–188
24. Granero AM, Fernández H, Agostini E, Zón MA (2010) Talanta 83: 249–255
25. Apetreia C, Rodríguez-Méndezb ML, De Sajac JA (2011) Electrochim Acta 56:8919–8925
26. Fan Q, Shan D, Xue H, He Y, Cosnier S (2007) Biosens Bioelectron 22:816–821
27. Singh S, Jain DVS, Singla ML (2013) Sensor Actuators B 182: 161–169
28. Kochana J, Gala A, Parczewski A, Adamski J (2008) Anal Bioanal Chem 391:1275–1281
29. Chawla S, Rawal R, Sharma S, Pundir CS (2012) Biochem Eng J 68:76–84
30. Arecchi A, Scampicchio M, Drusch S, Mannino S (2010) Anal Chim Acta 659:133–136
31. Aihua L, Itaru H, Haoshen Z (2005) Electrochem Commun 7:233–236
32. Karim F, Fakhruddin ANM (2012) Rev Environ Sci Biotechnol 11: 261–274
33. Lu LM, Zhang L, Zhang XB, Huan SY, Shen GL, Yu RQ (2010) Anal Chim Acta 665:146–151
34. Zhao JW, Wu DH, Zhi JF (2009) Bioelectrochemistry 75:44–49
35. Janegitz Bruno C, Medeiros Roberta A, Rocha-Filho Romeu C (2012) Fatibello-Filho Orlando. Diam Relat Mater 25:128–133
36. Zou YS, He LL, Zhang YC, Li ZX, Wang HP, Gu L, Tu CJ, Zeng HB (2013) Mater Chem Phys 141:851–821
37. Wang YG, Lau SP, Tay BK, Zhang XH (2002) J Appl Phys 92: 7253–7256
38. Zhang GJ, Song KS, Nakamura Y, Ueno T, Funatsu T, Ohdomari I, Kawarada H (2006) Langmuir 22:3728–3734
39. Torrengo S, Miotello A, Minati L, Bernagozzi I, Ferrari M, Dipalo M, Kohn E, Speranza G (2011) Diam Relat Mater 20:990–994
40. Zhuang H, Srikanth Vadali VSS, Jiang X, Luo J, Ihmels H, Aronov I, Wenclawiak BW, Adlung M, Wickleder C (2009) Appl Phys Lett 95:143703
41. Zhou YL, Tian RH, Zhi JF (2007) Biosens Bioelectron 22:822–828
42. Zhou YL, Zhi JF (2006) Electrochem Commun 8:1811–1816
43. Liu Z, Liu B, Kong J, Deng J (2000) Anal Chem 72:4707–4712
44. Wang SF, Tan YM, Zhao DM, Liu GD (2008) Biosens Bioelectron 23:1781–1787
45. Lu LM, Zhang L, Zhang XB, Huan SY, Shen GL, Yu RQ (2001) Anal Chim Acta 665:146–151
46. Rajesh KK (2005) Curr Appl Phys 5:178–183
47. Wang B, Zhang J, Dong S (2000) Biosens. Bioelectron 15:397–402
48. Kim MA, Lee WY (2003) Anal Chim Acta 479:143–150